ChemComm

COMMUNICATION

View Article Online
View Journal | View Issue



Cite this: *Chem. Commun.*, 2015, 51, 4465

Received 24th December 2014,
Accepted 4th February 2015

DOI: 10.1039/c4cc10292d

www.rsc.org/chemcomm

# Self-assembled supramolecular cages containing ruthenium(II) polypyridyl complexes†

Jiajia Yang,[ab] Mohan Bhadbhade,[c] William A. Donald,[b] Hasti Iranmanesh,[b] Evan G. Moore,[d] Hong Yan[a] and Jonathon E. Beves*[ab]

**Substitution-inert, redox- and photo-active ruthenium(II) complexes based on 2,2′,6′,2″-terpyridine ligands were self-assembled into discrete supramolecular cages *via* coordination to palladium(II) centres and characterised by NMR, ESI-MS and X-ray crystallography.**

Ruthenium(II) polypyridyl complexes exhibit remarkable photophysical properties and stability,[1] continuing to find new applications including water splitting,[2] visible light photoredox processes[3] and biological imaging.[4] Many examples of ruthenium(II) polypyridines have been reported being incorporated into extended structures such as organic polymers,[5] vesicles,[6] coordination polymers[7] and networks,[8] as well as acting as photosensitizers for molecular machines[9] and as components of discrete 2D macrocycles[10] or related assemblies.[11] However, examples of 3D molecular cages[12–14] containing Ru(II) centres remain rare,[12,15] in part due to the inert nature of this low-spin $d^6$ complexes. Herein we report, to the best of our knowledge, the first structural characterisation of incorporation of the prototypical $[Ru(tpy)_2]^{2+}$ (tpy = 2,2′,6′,2″-terpyridine[16–18]) unit into a discrete 3D molecular cage.[19] Functionalised $[Ru(tpy)_2]^{2+}$ units are particularly appealing as only a single isomer of this complex is possible, in contrast to bidentate analogues such as $Ru(bpy)_3^{2+}$ (bpy = 2,2′-bipyridine), which greatly simplifies the number of possible species formed when linking multiple Ru(II) centres. Complexes $[Ru(\mathbf{1})_2]^{2+}$ and $[Ru(\mathbf{2})_2]^{2+}$ feature inert $[Ru(tpy)_2]^{2+}$ units decorated with pendant pyridyl groups capable of binding additional metal centres (Fig. 1).[20] Square planar Pd(II) complexes are well suited to binding pyridyl ligands to form metallosupramolecular structures, using approaches pioneered by Fujita[21] and Stang.[22] Reaction of $[Ru(\mathbf{1})_2](PF_6)_2$ with two equivalents of Pd(dppp)(OTf)$_2$ (dppp = 1,3-diphenylphosphinopropane) in nitromethane at room temperature (Fig. 2) immediately gave a single major species in solution, as characterised by $^1$H, $^{13}$C and $^{31}$P NMR (Fig. 3). This assembly appears quantitative by NMR. The four-fold symmetry of the parent complex (Fig. 3a) is maintained in the product indicating the formation of a highly symmetric species with all tpy ligands being equivalent. Significant changes in NMR chemical shifts and very considerable broadening of signals at room temperature are observed upon Pd(II) coordination. Variable temperature NMR confirmed room temperature to be close to the coalescence temperature (in $CD_3NO_2$ or $CD_3CN$). High temperature (348 K, Fig. 3c) $^1$H and heteronuclear 2D NMR experiments (see ESI,† Fig. S13–S17 for details) were used to unambiguously assign all proton and carbon NMR signals. The signals of the protons of the pendant pyridyl groups are shifted slightly upfield ($\Delta\delta$ $H^{D2}$ − 0.09; $H^{D3}$ − 0.17 ppm; Fig. 3a and b) upon coordination to the Pd(II) centre. However, the most significant changes in chemical shifts are for the signals of the terpyridine moiety, which is distant from the Pd(II) coordination site.

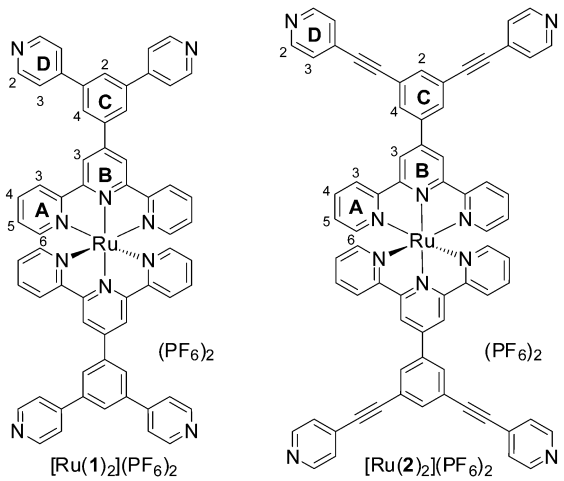


Fig. 1 Structure of complexes that are building blocks of more complex supramolecular cages, showing the numbering scheme adopted.

[a] *State Key Laboratory of Coordination Chemistry, School of Chemistry and Chemical Engineering, Nanjing University, Nanjing 210093, China*
[b] *School of Chemistry, The University of New South Wales (UNSW), Sydney, NSW 2052, Australia. E-mail: j.beves@unsw.edu.au*
[c] *Mark Wainwright Analytical Centre, The University of New South Wales (UNSW), Sydney, NSW 2052, Australia*
[d] *School of Chemistry and Molecular Biosciences, The University of Queensland, Brisbane, QLD 4072, Australia*

† Electronic supplementary information (ESI) available: Synthetic procedures, $^1$H, $^{13}$C, $^{31}$P, COSY, HSQC, HMBC, NOESY and variable temperature and variable concentration NMR spectra, X-ray crystal refinement details, ESI-MS and photophysical data. CCDC 1040284 and 1045515. For ESI and crystallographic data in CIF or other electronic format see DOI: 10.1039/c4cc10292d

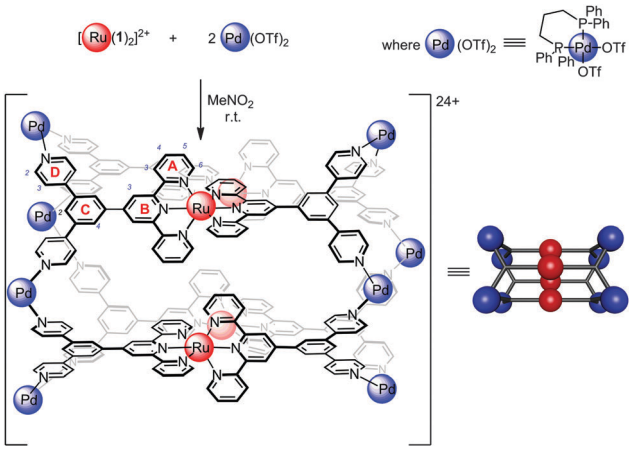


Fig. 2 Synthesis of molecular tetrameric cage $\mathbf{3}^{24+}$ from complex [Ru(**1**)$_2$](PF$_6$)$_2$ and Pd(dppp)(OTf)$_2$ in nitromethane or acetonitrile at room temperature within minutes.

Signals corresponding to the protons of the terminal pyridine ring (ring A, see Fig. 1 for labelling scheme) are shifted upfield ($\Delta\delta$ ppm: $H^{A3}$ − 0.46; $H^{A4}$ − 1.03; $H^{A5}$ − 1.34; $H^{A6}$ − 0.54) upon coordination with the Pd(II) corner units. These upfield shifts are consistent with the highly shielding environment expected within a molecular cage.[23] The $^{31}P\{^1H\}$ NMR spectrum (Fig. S8, ESI†) exhibited a single sharp singlet at 8.81 ppm for the dppp ligand, also supporting the high symmetry of the structure, in addition to the expected multiplet for the $PF_6^-$ anions (−144 ppm). The $^{13}C\{^1H\}$ spectrum (Fig. S7, ESI†) was fully assigned by 2D experiments (see Fig. S11, S12, S16 and S17, ESI†), including the two non-equivalent phenyl rings of the dppp ligand. The $^{13}C$ NMR signals showed characteristic peak shifts upon coordination to Pd(II), with signals of the $C^{D2}$ and $C^{D3}$ carbons ($\Delta\delta$ $C^{D2}$ − 0.6; $C^{D3}$ + 2.7; $C^{D4}$ − 3.1 ppm) and the carbons on the central phenyl ring ($\Delta\delta$ $C^{C1}$ + 2.1; $C^{C2}$ − 0.9; $C^{C4}$ + 1.2; $C^{C5}$ − 0.8 ppm) showing the largest shifts relative to Ru(**1**)$_2$(PF$_6$)$_2$.

Electrospray ionisation mass spectrometry (ESI-MS) of a nitromethane solution of the product resulted in the formation of a relatively abundant distribution of ions that were charged from +5 to +10 (Fig. 4). The difference in *m*/*z* values between adjacent ions in the distribution and the isotopic patterns were assigned to $[\mathbf{3}(PF_6^-)_{24-n}]^{n+}$ ($n$ = 5 to 10), formed by the sequential loss of $PF_6$ counter anions from [**3**(PF$_6$)$_{24}$] (11 742 Da; Fig. 4). This $Ru_4Pd_8$ tetrameric cage structure, [**3**](PF$_6$)$_{24}$, is the smallest least-strained structure possible for this system.[24] Additional peaks were observed corresponding to the loss of one $Pd(dppp)^{2+}$ unit which were confirmed by collision-induced dissociation (CID) experiments. This structure is also consistent with the broad $^1H$ NMR signals observed in solution, as the {Ru(tpy)$_2$} units rotate slowly on the NMR timescale and the environment inside and outside of the cage is non-equivalent. This restricted rotation is due to the close contact between the {Ru(tpy)$_2$} groups forming something resembling a poorly assembled gear box (see later X-ray structure discussion). Although stable in acetonitrile at high concentrations (>1 mM), based on $^1H$ NMR, the cage disassembles upon dissolution in acetonitrile (see Fig. S25, ESI†), which is not surprising given this solvent can act as an excellent ligand for Pd(II) centres. However, the complex was observed to be stable in pure nitromethane (Fig. S26, ESI†), a polar but very weakly coordinating solvent, over the same

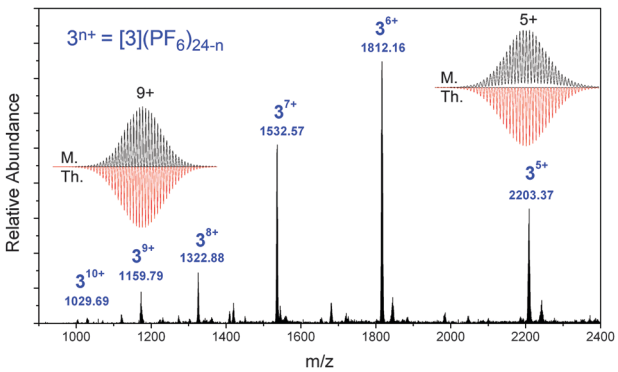


Fig. 4 ESI-MS an nitromethane solution containing cage [**3**](PF$_6$)$_{24}$. Inserts show the measured (top) and calculated (bottom) isotope patterns for the +9 and +5 peaks. Additional data is given in the supplementary information. Calculated mass for {Ru(**1**)$_2$}$_4${Pd(dppp)$_8$(PF$_6$)$_{24}$} = 11742.6 mass units.

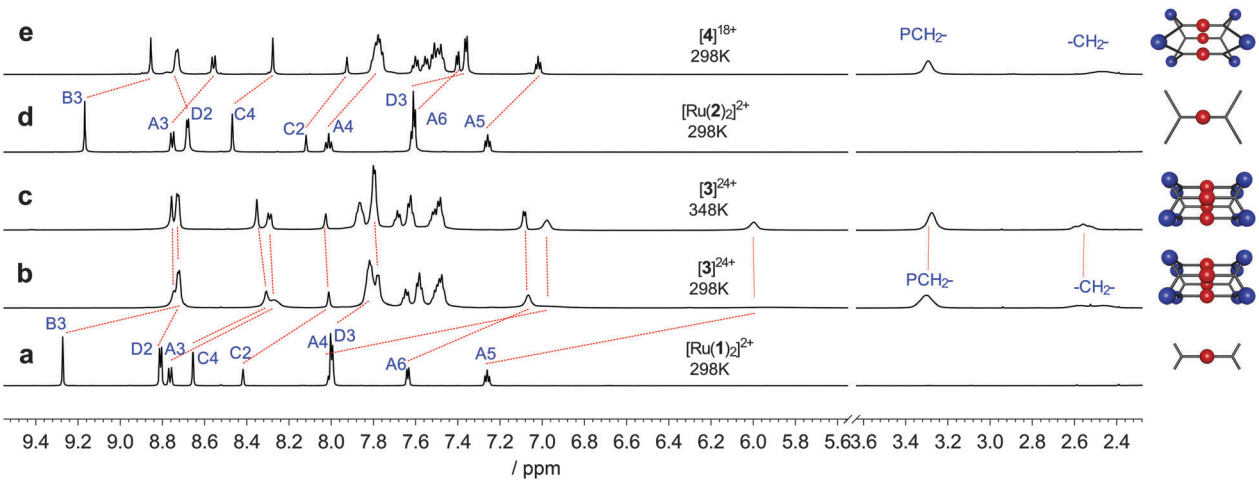


Fig. 3 $^1H$-NMR ($CD_3NO_2$, 600 MHz) spectra of (a) Ru(**1**)$_2$(PF$_6$)$_2$ 298 K; (b) cage **3** 298 K; (c) cage **3** 348 K; (d) Ru(**2**)$_2$(PF$_6$)$_2$ 298 K and (e) cage **4** 298 K. See Fig. 1 for labelling scheme. Peaks not labelled correspond to the two non-equivalent phenyl rings of the dppp ligand.

 

concentration range, confirming this solvent as an excellent choice for this class of metallosupramolecular systems.

The analogous reaction with complex $[Ru(\mathbf{2})_2](PF_6)_2$, which features alkyne spacers between the phenyl and pendant pyridyl rings, and $Pd(dppp)(OTf)_2$ also formed a single major product in solution (Fig. 5). The $^{31}P\{^1H\}$ spectrum (Fig. S29, ESI†) again revealed a single sharp singlet at 8.91 ppm, effectively identical to that observed for $[\mathbf{3}]^{24+}$, and consistent with the formation of a single major product. However, in contrast to cage $\mathbf{3}^{24+}$, the $^1H$ NMR signals (Fig. 3e) of this new species were not significantly broader than the parent $Ru(\mathbf{2})^{2+}$ complex, suggesting the rotation of $\{Ru(tpy)_2\}$ units was effectively unhindered in this structure. The $^1H$ NMR signals corresponding to the pendant pyridine protons were shifted relative to $[Ru(\mathbf{2})_2](PF_6)_2$ ($\Delta\delta$ $H^{D2}$ + 0.05; $H^{D3}$ − 0.32), but as was the case for cage $\mathbf{3}^{24+}$, the signals of the terpyridine group were significantly affected, all being shifted upfield ($\Delta\delta$ $H^{B3}$ − 0.31; $H^{A3}$ − 0.19; $H^{A4}$ − 0.26; $H^{A5}$ − 0.24; $H^{A6}$ − 0.28) but to a much less extent than in cage $\mathbf{3}^{24+}$. These peak shifts correspond to a cage environment considerably less shielded than in cage $\mathbf{3}^{24+}$. The $^{13}C\{^1H\}$ NMR spectrum (Fig. S28, ESI†) reveals relatively small changes in peak shifts for most signals, with the notable exceptions of the pendant pyridyl signals ($\Delta\delta$ $C^{D2}$ − 0.3; $C^{D3}$ + 2.7; $C^{D4}$ + 3.6 ppm), the alkynes ($\Delta\delta$ $C^{C}$–C≡C + 4.5 ppm; $C^{D}$–C≡C − 1.5 ppm) and the central phenyl ring ($\Delta\delta$ $C^{C1}$ − 1.6; $C^{C2}$ + 0.2; $C^{C4}$ + 2.0; $C^{C5}$ + 0.1 ppm). These peak shifts reflect not only the electronic effect of Pd(II) coordination to the pyridyl group, but also the strain introduced to the alkyne upon bending to form a smaller cyclic structure, hence the observed changes are significantly different to that observed for cage $\mathbf{3}^{24+}$.

The ESI-MS of a solution of this product (Fig. S36, ESI†) revealed a trimeric, rather than tetrameric structure, consistent with the structure of cage $\mathbf{4}(PF_6)_{18}$ (Fig. 5) indicating the additional flexibility of the alkyne spacers was sufficient to allow a smaller structure to form and simple molecular modelling (MMFF, Fig. S40, ESI†) supports this assignment. This structure was found to precipitate from solution (acetonitrile) over time to form an insoluble red powder, presumably a coordination polymer. In nitromethane the cage appears stable over several months in solution.

Slow diffusion of toluene into a nitromethane solution of cage $\mathbf{3}(PF_6)_{24}$ gave red block crystals suitable for X-ray diffraction.‡ The molecule crystallises in the $P\bar{1}$ space group with the asymmetric unit containing half of one cage molecule and disordered solvents and anions (Fig. 6). The complex forms a box-like structure approximately 21 × 21 × 32 Å in dimensions with Pd(II) centres at each end forming near perfect squares (Pd–Pd–Pd angles of 86.0–92.8° and Pd···Pd distances of 13.2–13.4 Å). The centre of the cage is occupied by $\{Ru(tpy)_2\}$ units with alternating Ru···Ru distances of 11.82 and 8.78 Å and inter-$\{Ru(tpy)_2\}$ pyridine···pyridine separations of (centroid···centroid) 3.86 and 5.34 Å forming portals which are occupied by $PF_6^-$ counterions. The cavities and each end of the cage are sufficiently large to potentially accommodate large guests such as a $C_{60}$ molecule. The $\{Ru(tpy)_2\}$ groups form pairs of terpyridine 'embraces'[25] (Fig. S37, ESI†), a type of favourable edge-to-face and face-to-face aromatic interactions, as often seen in solid state packing of simple $\{M(tpy)_2\}^{n+}$ complexes. These interactions reveal the origin of the restricted rotation of these units in solution. Although not requiring a concerted rotation of all the $\{Ru(tpy)_2\}$ units, it appears this type of

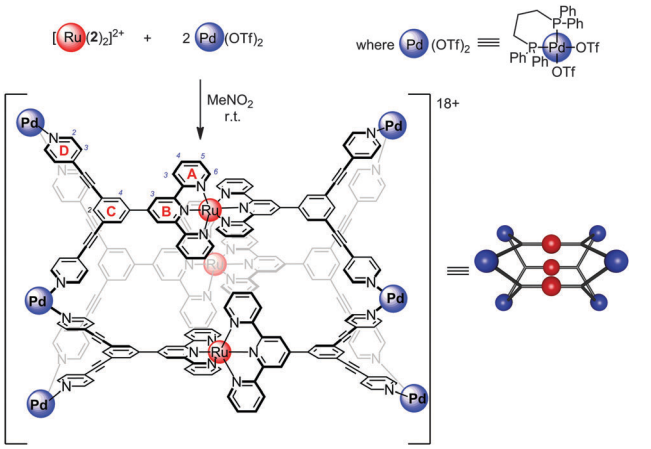


Fig. 5 Synthesis of molecular trimeric cage $\mathbf{4}^{24+}$ from complex $[Ru(\mathbf{2})_2](PF_6)_2$ and $Pd(dppp)(OTf)_2$ in nitromethane or acetonitrile at room temperature within minutes.

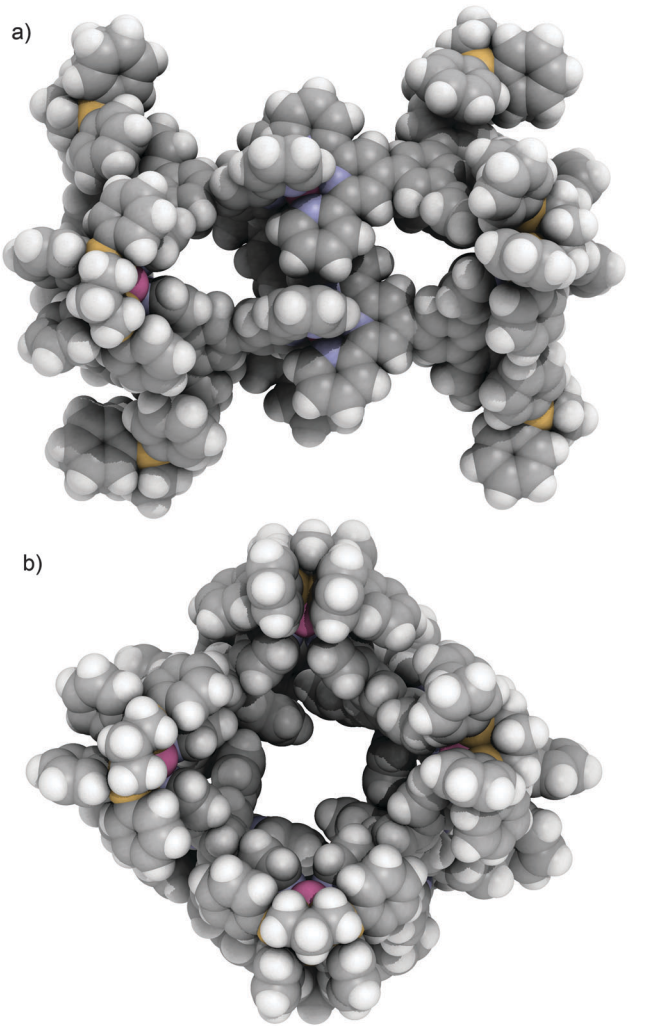


Fig. 6 The single crystal X-ray crystal structure of $[\mathbf{3}](PF_6)_{17.5}\cdot CH_3NO_2$. Viewed down the (a) crystallographic *a* axis, and (b) *c** axis. Solvent and anions omitted for clarity.

favourable π–π stacking interactions are more significant than simply steric crowding and result in the hindered rotation of these units. The cages are assembled together in the crystal structure *via* additional intermolecular terpyridine embraces to form 1D chain along the crystallographic *a* axis as well as extensive π–π interactions between the pyridine and phenyl rings along the *b* axis (Fig. S39, ESI†).

Preliminary investigations of the photophysical properties of cage $[\mathbf{3}](PF_6)_{24}$ indicate the functionality of the parent complex is retained in the cage structure. The $^1$MLCT absorption maxima of the $[Ru(\mathbf{1})_2](PF_6)_2$ [20] complex and cage $[\mathbf{3}](PF_6)_{24}$ were both located at 490 nm, while the $^3$MLCT emission spectra were essentially superimposable centred at 640 nm. The excited state lifetimes (1.26 ± 0.01 ns and 1.21 ± 0.01 ns respectively) were similarly identical, and are comparable to those of related [Ru(4′-tolyl-tpy)(tpytpy)]$^{2+}$ complexes (see ESI† for details).[26]

Three dimensional molecular cages containing $[Ru(tpy)_2]^{2+}$ units are reported and characterised in solution and the solid state. The photophysical properties of the parent Ru(II) complex $[Ru(\mathbf{1})_2]^{2+}$ are retained in the cage $\mathbf{3}^{24+}$, suggesting this new class of molecular cages may be potential candidates to act as photosensitizers for bound guest molecules. The introduction of an alkyne spacer, producing a larger ligand, resulted in the formation of a smaller, trimeric cage highlighting the flexibility of these spacer units and the subtlety of the assembly process.

This work was supported by a National Science Foundation of China (NSFC) Research Fund for International Young Scientists Project (No. 21450110060 and 21271102). The Australian Research Council is acknowledged for Future Fellowship (EGM, FT100100795) and Discovery Early Career Research Awards (WAD, DE130100424). Photophysical measurements were undertaken at the Photochemistry and Ultrafast Laser Spectroscopy (PULSΞ) facility, School of Chemistry and Molecular Biosciences, with financial support from the University of Queensland (MEI-2013000106). Crystallographic data was collected in-house at UNSW, or at the MX1 beamline at the Australian Synchrotron under a Collaborative Access Program (AS143_MXCAP_8503).

## Notes and references

‡ Crystal data and refinement: $C_{232}H_{188}N_{20}P_8Pd_4Ru_2{\cdot}8.75(F_6P){\cdot}0.5(CNO_2)$, $M$ = 5429.01, $T$ = 150(2) K, $\lambda$ = 0.71073 Å, triclinic, space group $P\bar{1}$, $a$ = 23.8865 (13), $b$ = 25.4288 (13), $C$ = 31.7818 (17) (Å), $\alpha$ = 96.150 (3), $\beta$ = 107.106 (3), $\gamma$ = 113.591 (2) (°), $V$ (Å$^3$) = 16341.8 (16), $Z$ = 2, m (mm$^{-1}$) = 0.46, $F(000)$ = 5460.5, data/restr/param. 57493/1988/3008. GOOF on $F^2$ = 1.11, $R[F^2 > 2s(F^2)]$ = 0.113, w$R(F^2)$ = 0.320. CCDC reference number 1040284.

1 S. Campagna, F. Puntoriero, F. Nastasi, G. Bergamini and V. Balzani, in *Photochemistry and Photophysics of Coordination Compounds I*, ed. V. Balzani and S. Campagna, Springer-Verlag Berlin, Berlin, 2007, vol. 280, pp. 117–214.
2 (*a*) W. J. Youngblood, S.-H. A. Lee, Y. Kobayashi, E. A. Hernandez-Pagan, P. G. Hoertz, T. A. Moore, A. L. Moore, D. Gust and T. E. Mallouk, *J. Am. Chem. Soc.*, 2009, **131**, 926–927; (*b*) L. Duan, F. Bozoglian, S. Mandal, B. Stewart, T. Privalov, A. Llobet and L. Sun, *Nat. Chem.*, 2012, **4**, 418–423.
3 D. M. Schultz and T. P. Yoon, *Science*, 2014, **343**, 985.
4 V. Fernandez-Moreira, F. L. Thorp-Greenwood and M. P. Coogan, *Chem. Commun.*, 2010, **46**, 186–202.
5 Y. Sun, Z. Chen, E. Puodziukynaite, D. M. Jenkins, J. R. Reynolds and K. S. Schanze, *Macromolecules*, 2012, **45**, 2632–2642.
6 P. Mahato, S. Saha, S. Choudhury and A. Das, *Chem. Commun.*, 2011, **47**, 11074–11076.
7 (*a*) J. E. Beves, E. C. Constable, C. E. Housecroft, C. J. Kepert and D. J. Price, *CrystEngComm*, 2007, **9**, 456–459; (*b*) J. E. Beves, E. C. Constable, C. E. Housecroft, C. J. Kepert, M. Neuburger, D. J. Price, S. Schaffner and J. A. Zampese, *Dalton Trans.*, 2008, 6742–6751; (*c*) J. E. Beves, E. C. Constable, S. Decurtins, E. L. Dunphy, C. E. Housecroft, T. D. Keene, M. Neuburger and S. Schaffner, *CrystEngComm*, 2008, **10**, 986–990; (*d*) J. E. Beves, D. J. Bray, J. K. Clegg, E. C. Constable, C. E. Housecroft, K. A. Jolliffe, C. J. Kepert, L. F. Lindoy, M. Neuburger, D. J. Price, S. Schaffner and F. Schaper, *Inorg. Chim. Acta*, 2008, **361**, 2582–2590.
8 (*a*) M. S. Deshpande, A. S. Kumbhar, V. G. Puranik and K. Selvaraj, *Cryst. Growth Des.*, 2006, **6**, 743–748; (*b*) C. A. Kent, D. Liu, L. Ma, J. M. Papanikolas, T. J. Meyer and W. Lin, *J. Am. Chem. Soc.*, 2011, **133**, 12940–12943; (*c*) R. W. Larsen and L. Wojtas, *J. Phys. Chem. A*, 2012, **116**, 7830–7835; (*d*) T. Toyao, M. Saito, S. Dohshi, K. Mochizuki, M. Iwata, H. Higashimura, Y. Horiuchi and M. Matsuoka, *Chem. Commun.*, 2014, **50**, 6779–6781.
9 (*a*) V. Balzani, G. Bergamini, F. Marchioni and P. Ceroni, *Coord. Chem. Rev.*, 2006, **250**, 1254–1266; (*b*) S. Bonnet and J.-P. Collin, *Chem. Soc. Rev.*, 2008, **37**, 1207–1217.
10 (*a*) S.-S. Sun and A. J. Lees, *Inorg. Chem.*, 2001, **40**, 3154–3160; (*b*) G. R. Newkome, T. J. Cho, C. N. Moorefield, R. Cush, P. S. Russo, L. A. Godínez, M. J. Saunders and P. Mohapatra, *Chem. – Eur. J.*, 2002, **8**, 2946–2954; (*c*) G. R. Newkome, T. J. Cho, C. N. Moorefield, P. P. Mohapatra and L. A. Godínez, *Chem. – Eur. J.*, 2004, **10**, 1493–1500; (*d*) A. Schultz, X. Li, B. Barkakaty, C. N. Moorefield, C. Wesdemiotis and G. R. Newkome, *J. Am. Chem. Soc.*, 2012, **134**, 7672–7675.
11 M. W. Cooke and G. S. Hanan, *Chem. Soc. Rev.*, 2007, **36**, 1466–1476.
12 For a recent example of a molecular cage prepared with Ru(II) polypyridyl complexes with Pd(II) ions, see: K. Li, L.-Y. Zhang, C. Yan, S.-C. Wei, M. Pan, L. Zhang and C.-Y. Su, *J. Am. Chem. Soc.*, 2014, **136**, 4456–4459.
13 For examples of cages featuring Ru(II) organometallics, see (*a*) B. Therrien, G. Süss-Fink, P. Govindaswamy, A. K. Renfrew and P. J. Dyson, *Angew. Chem., Int. Ed.*, 2008, **47**, 3773–3776; (*b*) A. Granzhan, T. Riis-Johannessen, R. Scopelliti and K. Severin, *Angew. Chem., Int. Ed.*, 2010, **49**, 5515–5518; (*c*) L. Wang, J.-F. Liu, W. Yang, F.-Y. Yi, S. Dang and Z.-M. Sun, *Dalton Trans.*, 2014, **43**, 17244–17247.
14 For leading examples of functional molecular cages, see (*a*) M. D. Pluth, R. G. Bergman and K. N. Raymond, *Science*, 2007, **316**, 85–88; (*b*) P. Mal, B. Breiner, K. Rissanen and J. R. Nitschke, *Science*, 2009, **324**, 1697–1699; (*c*) Y. Inokuma, M. Kawano and M. Fujita, *Nat. Chem.*, 2011, **3**, 349–358.
15 For recent examples of cages containing Ru(II) and pyridyl ligands, see (*a*) A. J. Metherell and M. D. Ward, *Chem. Commun.*, 2014, **50**, 6330–6332; (*b*) A. J. Metherell and M. D. Ward, *Chem. Commun.*, 2014, **50**, 10979–10982.
16 E. C. Constable, *Chem. Soc. Rev.*, 2007, **36**, 246–253.
17 It should be noted that the excited state properties of $[Ru(tpy)_2]^{2+}$ are limited compared to $[Ru(bpy)_3]^{2+}$, for details see: A. K. Pal and G. S. Hanan, *Chem. Soc. Rev.*, 2014, **43**, 6184–6197.
18 For a recent examples of a terpyridine containing molecular cages, see (*a*) C. Wang, X.-Q. Hao, M. Wang, C. Guo, B. Xu, E. N. Tan, Y.-Y. Zhang, Y. Yu, Z.-Y. Li, H.-B. Yang, M.-P. Song and X. Li, *Chem. Sci.*, 2014, **5**, 1221–1226; (*b*) X. Lu, X. Li, K. Guo, T.-Z. Xie, C. N. Moorefield, C. Wesdemiotis and G. R. Newkome, *J. Am. Chem. Soc.*, 2014, **136**, 18149–18155.
19 For a recent example of a molecular cage containing $[Ru(tpy)_2]^{2+}$ formed under kinetic control and characterised by NMR and ESI-MS, see: T.-Z. Xie, S.-Y. Liao, K. Guo, X. Lu, X. Dong, M. Huang, C. N. Moorefield, S. Z. D. Cheng, X. Liu, C. Wesdemiotis and G. R. Newkome, *J. Am. Chem. Soc.*, 2014, **136**, 8165–8168.
20 J. Yang, J. K. Clegg, Q. Jiang, X. Lui, H. Yan, W. Zhong and J. E. Beves, *Dalton Trans.*, 2013, **42**, 15625–15636.
21 (*a*) M. Fujita, J. Yazaki and K. Ogura, *J. Am. Chem. Soc.*, 1990, **112**, 5645–5647; (*b*) M. Fujita, M. Tominaga, A. Hori and B. Therrien, *Acc. Chem. Res.*, 2005, **38**, 369–378.
22 (*a*) P. J. Stang, D. H. Cao, S. Saito and A. M. Arif, *J. Am. Chem. Soc.*, 1995, **117**, 6273–6283; (*b*) R. Chakrabarty, P. S. Mukherjee and P. J. Stang, *Chem. Rev.*, 2011, **111**, 6810–6918.
23 W. Meng, B. Breiner, K. Rissanen, J. D. Thoburn, J. K. Clegg and J. R. Nitschke, *Angew. Chem., Int. Ed.*, 2011, **50**, 3479–3483.
24 Self-assembled systems tend to form the smallest least-strained species on entropy grounds. For a detailed discussion see C. Piguet, *Chem. Commun.*, 2010, **46**, 6209–6231.
25 For a detailed analysis of tpy embraces, see (*a*) J. McMurtrie and I. Dance, *CrystEngComm*, 2005, **7**, 216–229; (*b*) J. McMurtrie and I. Dance, *CrystEngComm*, 2009, **11**, 1141–1149.
26 E. G. Moore, M. Benaglia, G. Bergamini and P. Ceroni, *Eur. J. Inorg. Chem.*, 2015, 414–420.

 